A class of spline functions for landmark-based image registration

A class of spline functions for landmark-based image registration

G. Allasia, R. Cavoretto and A. De Rossi*

Abstract

A class of spline functions, called Lobachevsky splines, is proposed for landmark-based image registration. Analytic expressions of Lobachevsky splines and some of their properties are given, reasoning in the context of probability theory. Since these functions have simple analytic expressions and compact support, landmark-based transformations can be advantageously defined using them. Numerical results point out accuracy and stability of Lobachevsky splines, comparing them with Gaussians and thin plate splines. Moreover, an application to a real-life case (cervical X-ray images) shows the effectiveness of the proposed method.

Keywords: interpolation; image processing; landmark-based transformations; Lobachevsky splines; elastic registration; radial basis functions.

1 Introduction

The problem of image registration, one of the challenging problems in image processing, consists essentially in finding a suitable transformation between two images (or image data), called the *source* and the *target images*. More precisely, given two images, taken either at different times or from different devices or perspective, the aim is to determine a reasonable transformation, such that the transformed version of the first image is similar to the second image. There is a large number of application areas which demand registration, including astronomy, astrophysics, geophysics, computer vision, robotics and medicine, to name a few. For an overview, see e.g. [5, 19, 18, 21, 22, 30] and references therein. More specific examples include imaging techniques, such as computer tomography (CT) and magnetic resonance imaging (MRI).

The image registration process may be based on a finite set of landmarks, i.e. sparse data points located on images, usually not uniformly distributed. The basic idea is to find a transformation function $\mathbf{F} : \mathbb{R}^m \to \mathbb{R}^m$, where m is the image dimension, such that each landmark of the source image is mapped onto the corresponding landmark of the target image (see, e.g., [21, 22, 26]).

This problem can be formulated in the context of multivariate scattered data interpolation and solved by using radial basis functions (RBFs) (see, e.g., [10, 31]), in particular, thin plate splines. Their use was first proposed by Bookstein [3] and they are still commonly used (see the recent papers [23, 24] and the software package MIPAV [20]). Since RBFs are in general globally supported and a single landmark pair change may influence the whole registration result, in the last decade several methods have been proposed to circumvent this disadvantage, such as compactly supported RBFs [12], elastic body splines [14], and the modified inverse distance weighted method [6, 7].

In this paper we propose the use of a class of spline functions, called *Lobachevsky splines* (see [1, 8]), for landmark-based registration. We consider the analytic expressions of Lobachevsky splines and some of their properties, reasoning in the context of probability theory, which

*Department of Mathematics "G. Peano", University of Torino, via Carlo Alberto 10, I–10123 Torino, Italy. E-mail: giampietro.allasia@unito.it, roberto.cavoretto@unito.it, alessandra.derossi@unito.it

provides the most powerful tools. These splines can be used for multivariate scattered data interpolation, since they and their products are strictly positive definite functions. Moreover, Lobachevsky splines have simple analytic expressions and compact support, providing sparse interpolation matrices and the possibility of a fast evaluation. These interpolation matrices have also generally much smaller condition numbers than those given by Gaussian function. Numerical results for interpolation show accuracy of Lobachevsky splines, comparing them with the Gaussian. Hence, taking into consideration all the described properties, we define landmark-based transformations using Lobachevsky splines, which, as far as we know, have never been used in the image registration context before our sketch in [2]. In fact, [2] is only an extended abstract in which the topic is just sketched. Here instead we provide a complete and extensive presentation of Lobachevsky splines. In particular, we describe in detail properties and characteristics of Lobachevsky splines, referring not only to convergence properties but also giving an integral characterization of positive definiteness of Lobachevsky splines. Moreover, after considering the connection between Lobachevsky spline interpolation and image transformation, we report several numerical results testing on four typical test cases accuracy and effectiveness of Lobachevsky splines compared to Gaussian and thin plate spline. Finally, we show experimental results obtained by a real application to cervical X-ray images. Using Lobachevsky spline transformations, we obtained good results in both the test cases and in the real-life case application to cervical X-ray images. In particular, Lobachevsky splines achieve better results than Gaussians, with regard to accuracy and stability, and their performance is comparable with that of thin plate splines.

In Section 2 some preliminary definitions and the mathematical formulation of the landmark-based registration problem are given. In Section 3 we consider the analytic expressions of the Lobachevsky splines and some of their properties, discussing the strictly positive definiteness of such functions for univariate and multivariate interpolation. Section 4 is devoted to the formulation of the Lobachevsky spline transformations. Finally, in Section 5 several numerical results obtained for some test cases are presented, while in Section 6 an application to X-ray images is given.

2 Landmark-based registration problem

Let $\mathcal{S}_N = \{\mathbf{x}_j \in \mathbb{R}^m, j = 1, 2, \ldots, N\}$ be a given set of landmarks in the source image S and let $\mathcal{T}_N = \{\mathbf{t}_j \in \mathbb{R}^m, j = 1, 2, \ldots, N\}$ be the given set of corresponding landmarks in the target image T. The registration problem reads as follows.

Problem 2.1. *Let the landmark sets $\mathcal{S}_N$ and $\mathcal{T}_N$ be given. Find a transformation $\mathbf{F} : \mathbb{R}^m \to \mathbb{R}^m$ within a suitable space $\mathcal{F}$ of admissible functions, such that*

$$\mathbf{F}(\mathbf{x}_j) = \mathbf{t}_j, \qquad j = 1, 2, \ldots, N.$$

Each coordinate of the transformation function is calculated separately, i.e. the interpolation problem $F_k : \mathbb{R}^m \to \mathbb{R}$ is solved for each coordinate $k = 1, 2, \ldots, m$, with the corresponding conditions

$$F_k(\mathbf{x}_j) = t_{k,j}, \qquad j = 1, 2, \ldots, N. \tag{1}$$

In accordance with [18] we give also the following preliminary definitions.

Definition 2.1. *An image transformation is called rigid when only translations and rotations are allowed. If the transformation maps parallel lines onto parallel lines, it is called affine. If it maps lines onto lines, it is called projective. Finally, if it maps lines onto curves, it is called elastic.*

Definition 2.2. *An image transfomation is called global if it applies to the entire image, and local if each subsection of the image has its own defined transformation.*

3 Lobachevsky spline functions

3.1 Definitions and properties

Let us consider an infinite sequence $X_1, X_2, \ldots$ of random variables, which are independent and uniformly distributed on $[-a, a]$, $a \in \mathbb{R}^+$. The reduced sum of the first n variables

$$S_n^* = \frac{X_1 + X_2 + \cdots + X_n}{a\sqrt{\frac{n}{3}}}$$

satisfies the local form of the central limit theorem (see, e.g., [13, 25]), namely the sequence $f_n^*(x)$, $n = 1, 2, \ldots$, of the density functions of the random variables S_n^* converges to the normal density function with expectation 0 and standard deviation 1, i.e.

$$\lim_{n\to\infty} f_n^*(x) = \frac{1}{\sqrt{2\pi}} \exp\left(\frac{-x^2}{2}\right), \tag{2}$$

and moreover the convergence is uniform for all $x \in \mathbb{R}$.

To get an explicit expression of f_n^* it is convenient referring to the sum

$$S_n = a\sqrt{\frac{n}{3}} S_n^* = X_1 + X_2 + \cdots + X_n,$$

whose density function is denoted by $f_n(x)$. Since $S_n = X_n + S_{n-1}$ and X_n and S_{n-1} are independent, $f_n(x)$ is given by the convolution product

$$f_n(x) = \int_{-\infty}^{+\infty} f_1(u) f_{n-1}(x-u)du = \frac{1}{2a}\int_{-a}^{+a} f_{n-1}(x-u)du,$$

because by definition the density function of X_n is $f_1(x) = 1/(2a)$ for $-a \le x \le +a$ and $f_1(x) = 0$ elsewhere. Setting $x - u = t$, we get the recursive formula

$$f_n(x) = \frac{1}{2a}\int_{x-a}^{x+a} f_{n-1}(t)dt, \qquad n = 2, 3, \ldots \tag{3}$$

From (3) it follows for $-na \le x \le na$ ($f_n(x) = 0$ elsewhere)

$$\begin{aligned} f_n(x) &= \frac{1}{(2a)^n(n-1)!}\Big\{(x+na)^{n-1} - \binom{n}{1}[x+(n-2)a]^{n-1} \\ &+ \binom{n}{2}[x+(n-4)a]^{n-1} - \binom{n}{3}[x+(n-6)a]^{n-1} \\ &+ \binom{n}{4}[x+(n-8)a]^{n-1} - \binom{n}{5}[x+(n-10)a]^{n-1} + \ldots\Big\} \end{aligned} \tag{4}$$

where the sum is extended to all arguments $x + (n-2k)a$, $k = 0, 1, 2, \ldots$, which are positive. This result, which was found by Lobachevsky [15] (see [13, 25]), can be proved by induction, together with the property that $f_n(x)$ is an even function (see [11]).

Sometimes it may be convenient to consider different forms of (4), namely

$$f_n(x) = \frac{1}{(2a)^n(n-1)!}\sum_{k=0}^{\left\lfloor\frac{na+x}{2a}\right\rfloor}(-1)^k\binom{n}{k}[x+(n-2k)a]^{n-1},$$

where $\lfloor\cdot\rfloor$ means the greatest integer less than or equal to the argument, or

$$f_n(x) = \frac{1}{(2a)^n(n-1)!}\sum_{k=0}^{n}(-1)^k\binom{n}{k}[x+(n-2k)a]_+^{n-1}, \tag{5}$$

where the truncated power function $(x)_+$ is defined as x for $x > 0$ and 0 for $x \le 0$.

Note that classic B-splines with equally spaced knots are directly connected to Lobachevsky splines. To show it, we observe that the random variables $T_i = (X_i + a)/(2a),\ i = 1, 2, \ldots$, are uniformly distributed on $[0, 1]$ and the sum of the first n of them is

$$U_n \equiv \sum_{i=1}^{n} T_i = \sum_{i=1}^{n} \frac{X_i + a}{2a} = \frac{1}{2a} S_n + \frac{n}{2}.$$

Then, the density function $u_n(t)$ of U_n is given by

$$u_n(t) = 2a f_n\Big[2a\Big(t - \frac{n}{2}\Big)\Big] = \frac{1}{(n-1)!} \sum_{k=0}^{n} (-1)^k \binom{n}{k} (t-k)_+^{n-1},$$

which is a well-known form of the classic B-splines on the support $[0, n]$ (see, e.g. [27]). Like B-splines, Lobachevsky splines satisfy a three-term recurrence relation, namely,

$$f_n(x) = \frac{1}{n-1}\Big[\frac{na + x}{2a} f_{n-1}(x + a) + \frac{na - x}{2a} f_{n-1}(x - a)\Big], \tag{6}$$

which may be interesting from a computational point of view. In fact, this relation is very stable, whereas (5) could suffer from loss-of-significance errors owing to subtraction of nearly equal quantities.

The piecewise function $f_n(x)$ is graphically represented by polynomial arcs of degree $n - 1$; the first $n - 2$ derivatives of different polynomial arcs are equal at the knots (the points where the parabolic pieces are joined), i.e. $f_n \in C^{n-2}[-na, na]$. The knots are uniformly spaced with size $2a$, and $f_n(x)$ is an even function with support $[-na, na]$. In the case $a = 1/2$ the knots are unit spaced. This class of splines enjoys very interesting applications in signal and image processing, wavelets theory, etc. (see, e.g., [4, 9, 29]).

From a computational viewpoint it is convenient to evaluate $f_n(x)$ starting from the pieces defined on $[-na, 0]$ and then obtain the pieces on $[0, na]$ by symmetry. Moreover, each piece on $[-na, 0]$ can be obtained by the preceding one by simply adding a term, as clearly appears from (4).

Considering the connection between $f_n(x)$ and $f_n^*(x)$, the limit (2) becomes

$$\lim_{n\to\infty} f_n^*(x) = \lim_{n\to\infty} a\sqrt{\frac{n}{3}}\ f_n\Big(a\sqrt{\frac{n}{3}}\ x\Big) = \frac{1}{\sqrt{2\pi}} \exp\Big(\frac{-x^2}{2}\Big). \tag{7}$$

The variables S_n^* and S_n are said to be asymptotically normal $(0, 1)$ and $(0, a\sqrt{n/3})$, respectively.

Noteworthy convergence properties are also satisfied by integrals and derivatives of Lobachevsky splines. From the central limit theorem for the convergence in distribution (see, e.g., [25]) we have, referring to the distribution function of S_n^*,

$$\lim_{n\to\infty} \int_{-\infty}^{x} f_n^*(t)dt = \lim_{n\to\infty} \int_{-\infty}^{x} a\sqrt{\frac{n}{3}}\ f_n\Big(a\sqrt{\frac{n}{3}}\ t\Big)dt = \int_{-\infty}^{x} \frac{1}{\sqrt{2\pi}} \exp\Big(\frac{-t^2}{2}\Big)dt.$$

This result is also a direct consequence of (2) and Lebesgue's dominated convergence theorem.

The asymptotic behaviour of derivatives of Lobachevsky splines is described by the following result (see [4]).

Theorem 3.1. *The sequence $D^k f_n^*(x),\ n = 1, 2, \ldots$, of the k-th derivatives of $f_n^*(x)$, where $k \le n - 2$ is a fixed integer, converges to the k-th derivative of the standardized normal density function, i.e.,*

$$\lim_{n\to\infty} D^k f_n^*(x) = \lim_{n\to\infty} D^k\Big[a\sqrt{\frac{n}{3}}\ f_n\Big(a\sqrt{\frac{n}{3}}\ x\Big)\Big] = D^k\Big[\frac{1}{\sqrt{2\pi}} \exp\Big(\frac{-x^2}{2}\Big)\Big].$$

3.2 Integral characterizations of positive definiteness

A celebrated result on positive definite functions is given by Bochner's theorem (see, e.g., [10, 16]), whose characterization is expressed in terms of Fourier transforms.

Theorem 3.2 (**Bochner's theorem**). *A (complex-valued) function $\Phi \in C(\mathbb{R}^m)$ is positive definite on $\mathbb{R}^m$ if and only if it is the Fourier transform of a finite non-negative Borel measure μ on $\mathbb{R}^m$, i.e.*

$$\Phi(\mathbf{x}) = \frac{1}{\sqrt{(2\pi)^m}} \int_{\mathbb{R}^m} e^{-i(\mathbf{x}\cdot\mathbf{y})} d\mu(\mathbf{y}), \qquad \mathbf{x} \in \mathbb{R}^m,$$

where $(\mathbf{x} \cdot \mathbf{y})$ is the usual inner product.

If the measure μ is defined for any Borel set B by $\mu(B) = \int_B f(\mathbf{x})d\mathbf{x}$, then we get Corollary 3.1.

Corollary 3.1. *Let $f \in L_1(\mathbb{R}^m)$ be a continuous non-negative function, not identically zero. Then the Fourier transform of f is strictly positive definite on $\mathbb{R}^m$.*

Finally, a criterion to check whether a given function is strictly positive definite is reported in [31].

Theorem 3.3. *A continuous function $\Phi \in L_1(\mathbb{R}^m)$ is strictly positive definite if and only if Φ is bounded and its Fourier transform is non-negative and not identically equal to zero.*

Theorem 3.3 is of fundamental importance. In fact, if we assume that Φ is not identically equal to zero (which implies that also $\hat{\Phi}$ is not identically equal to zero), then we need to ensure only that $\hat{\Phi}$ be non-negative in order for Φ to be strictly positive definite.

3.3 Positive definiteness of Lobachevsky splines

To apply Bochner's theorem we need to know the characteristic functions of S_n and of related random variables. The characteristic function of X_i, $i = 1, 2, \ldots$, is

$$\frac{\sin(at)}{at}, \qquad t \in \mathbb{R}.$$

Since the random variables $X_1, X_2, \ldots, X_n$ are independent, the sum S_n has the characteristic function

$$\varphi_n(t) = \int_{-\infty}^{+\infty} \exp(itx) f_n(x) dx \left[\frac{\sin(at)}{at}\right]^n, \tag{8}$$

and, conversely,

$$f_n(x) = \frac{1}{2\pi} \int_{-\infty}^{+\infty} \exp(-itx)\varphi_n(t)dt = \frac{1}{2\pi} \int_{-\infty}^{+\infty} \exp(-itx) \left[\frac{\sin(at)}{at}\right]^n dt. \tag{9}$$

The characteristic function of S_n^* is from (8)

$$\varphi_n^*(t) = \left[\frac{\sin\left(t\sqrt{\frac{3}{n}}\right)}{t\sqrt{\frac{3}{n}}}\right]^n. \tag{10}$$

Let us consider the m-dimensional random vector $V_m = (Y_1, Y_2, \ldots, Y_m)$, $m \geq 2$, whose components are independent and have the same distribution as the sum S_n, so that the density

function of the vector V_m is $f_{V_m}(y_1, y_2, \ldots, y_m) = f_n(y_1) f_n(y_2) \cdots f_n(y_m)$. Then, the characteristic function of V_m is

$$\begin{aligned} \varphi_{V_m}(t_1, t_2, \ldots, t_m) &= \int_{\mathbb{R}^m} \exp\left(i \sum_{j=1}^{m} t_j y_j \right) f_{V_m}(y_1, y_2, \ldots, y_m) dy_1 dy_2 \cdots dy_m \\ &= \prod_{j=1}^{m} \varphi_n(t_j) = \prod_{j=1}^{m} \left[\frac{\sin(at_j)}{at_j} \right]^n, \end{aligned} \tag{11}$$

and, conversely,

$$\begin{aligned} f_{V_m}(y_1, y_2, \ldots, y_m) &= \frac{1}{(2\pi)^m} \int_{\mathbb{R}^m} \exp\left(-i \sum_{j=1}^{m} t_j y_j \right) \varphi_{V_m}(t_1, t_2, \ldots, t_m) dt_1 dt_2 \cdots dt_m \\ &= \frac{1}{(2\pi)^m} \int_{\mathbb{R}^m} \exp\left(-i \sum_{j=1}^{m} t_j y_j \right) \prod_{j=1}^{m} \left[\frac{\sin(at_j)}{at_j} \right]^n dt_1 dt_2 \cdots dt_m. \end{aligned}$$

The considered characteristic functions are strictly related to the *sinc function* (see, e.g., [17, 28])

$$\operatorname{sinc} t = \prod_{j=1}^{m} \frac{\sin(\pi t_j)}{\pi t_j}, \qquad t = (t_1, t_2, \ldots, t_m),$$

whose importance derives largely from its role in the sampling theorem (see, e.g., [9] and references therein).

It is well-known from probability theory that also the considered characteristic functions satisfy convergence properties. Precisely, we have from (10) and (11) respectively

$$\lim_{n\to\infty} \varphi_n^*(t) = \exp\left(\frac{-t^2}{2}\right), \quad \lim_{n\to\infty} \varphi_{V_m}^*(t_1, t_2, \ldots, t_m) = \exp\left(-\frac{1}{2}(t_1^2 + t_2^2 + \cdots + t_m^2) \right),$$

where the limit functions are the characteristic functions of the univariate and m-variate standardized normal distributions, and $\varphi_{V_m}^*(t_1, t_2, \ldots, t_m)$ is the characteristic function of the random vector V_m^* whose density function is $f_{V_m^*}(y_1, y_2, \ldots, y_m) = f_n^*(y_1) f_n^*(y_2) \cdots f_n^*(y_m)$. The former limit and Theorem 3.1 are interesting in the context of B-spline wavelets, which are strictly related to cardinal B-splines (see [4, 29]).

It is interesting to remark that also all the considered characteristic functions are strictly positive definite. In fact, every characteristic function is positive definite by Bochner's theorem and moreover in our case the theorem is applied considering continuous (for $n \geq 2$) and non-vanishing density functions.

Finally, we give the following theorem which allows us to construct multivariate (strictly) positive definite functions from univariate ones (see, e.g., [31]).

Theorem 3.4. *Suppose that $\phi_1, \phi_2, \ldots, \phi_m$ are (strictly) positive definite and integrable functions on $\mathbb{R}$, then*

$$\Phi(y) = \phi(y_1)\phi(y_2) \cdots \phi(y_m), \qquad y = (y_1, y_2, \ldots, y_m) \in \mathbb{R}^m,$$

is a (strictly) positive definite function on $\mathbb{R}^m$.

4 Lobachevsky spline transformations

4.1 Univariate and multivariate interpolation

Univariate interpolation on scattered data can be obtained by the operator

$$L_n(x) = \sum_{j=1}^{N} c_j f_n^*(x - x_j) = \sum_{j=1}^{N} d_j f_n(x - x_j), \qquad x, x_j; c_j, d_j \in \mathbb{R}, \tag{12}$$

where

$$f_n^*(x) = a\sqrt{\frac{n}{3}}\, f_n\left(a\sqrt{\frac{n}{3}}\, x\right),$$

f_n is given in (5) and n is even, because in this case f_n (and hence f_n^*) are strictly positive definite. On the one hand, the interpolant $L_n(x)$ is a linear combination of the shifted functions $f_n^*(x-x_j)$, which are spline functions with compact supports $[x_j-\sqrt{3n}, x_j+\sqrt{3n}]$ and continuous up to order $n-2$. On the other hand, $L_n(x)$ is a linear combination (with different coefficients d_j) of the shifted functions $f_n(x-x_j)$, whose compact supports are $[x_j-na, x_j+na]$. Increasing the degree n does not give rise to the oscillatory phenomenon typical of high degree polynomials, but the use of very high degree splines does not appear computation-wise convenient.

In general, for dimension $m \geq 2$, we have

$$L_n(\mathbf{x}) = L_n(x_1, x_2, \ldots, x_m) = \sum_{j=1}^{N} c_j f_n^*(x_1 - x_{1j}) f_n^*(x_2 - x_{2j}) \cdots f_n^*(x_m - x_{mj})$$

$$= \sum_{j=1}^{N} d_j f_n(x_1 - x_{1j}) f_n(x_2 - x_{2j}) \cdots f_n(x_m - x_{mj}), \tag{13}$$

where n is even, $c_j, d_j \in \mathbb{R}$, $(x_1, x_2, \ldots, x_m) \in \mathbb{R}^m$, and $(x_{1j}, x_{2j}, \ldots, x_{mj}) \in \mathbb{R}^m$, $j = 1, 2, \ldots, N$, are the data sites.

The coefficients c_j (or d_j) in (13) are well defined real numbers for any n, since they are the unique solution of a linear system, but they change in general with n. When n becomes very large we have by (7) asymptotically

$$L_n(x_1, x_2, \ldots, x_m) \asymp \frac{1}{(2\pi)^{m/2}} \sum_{j=1}^{N} \exp\left[-\frac{1}{2}\sum_{i=1}^{m}(x_i - x_{ij})^2\right]$$

for any $(x_1, x_2, \ldots, x_m) \in \mathbb{R}^m$ and fixed $(x_{1j}, x_{2j}, \ldots, x_{mj}) \in \mathbb{R}^m$. Hence, it occurs that $L_n(x_1, x_2, \ldots, x_m)$ gives an asymptotically radial approximation and its numerical performance turns out to be comparable with the one of the Gaussian function. We observe that $L_n(x_1, x_2, \ldots, x_m)$ has a simple analytic expression, that its interpolation matrix is sparse with a condition number smaller than the Gaussian one, and that the recurrence relation (6) is a valid alternative to (5). Moreover, Lobachevsky splines are more efficient than Gaussians and thin plate splines, because: (i) sparsity of Lobachevsky spline interpolation matrices allows us to use "ad hoc" techniques for solving the associated linear systems, thus achieving a considerable saving of memory and computational effort; (ii) Lobachevsky splines (as well as Gaussians) need to solve linear sistems of dimension $N \times N$, while thin plate splines require the solution of linear systems of dimension $(N+3) \times (N+3)$ since, in order to have positive definite matrices, the addition of a polynomial term of degree one is necessary (see [10]).

Remark 4.1. *It is well-known that using Gaussians the introduction of a shape parameter α is convenient. This trick can suitably be applied also in our case considering $f_n^*(\alpha x)$. Using the shape parameter as a factor we observe that a decrease of the shape parameter produces flat basis functions, while increasing α leads to more peaked (or localized) basis functions. The same result can be achieved considering $f_n(x)$ and acting on the parameter a. Numerical computations show that the approximation performances obtained by $f_n^*(x)$ or $f_n(x)$ are practically equivalent, if the values of the parameters α and a are suitably chosen [1, 8].*

4.2 Definition of Lobachevsky spline transformations

Let us consider the following definition of the Lobachevsky spline transformation, formulated in the context of image registration.

Definition 4.1. *Given a set of source landmark points* $\mathcal{S}_N = \{\mathbf{x}_j \in \mathbb{R}^m, j = 1, 2, \ldots, N\}$*, with the associated corresponding set of target landmark points* $\mathcal{T}_N = \{\mathbf{t}_j \in \mathbb{R}^m, j = 1, 2, \ldots, N\}$*, a Lobachevsky spline transformation* $\mathbf{L}_n : \mathbb{R}^m \to \mathbb{R}^m$ *is such that each one of its components*

$$(L_n)_k : \mathbb{R}^m \to \mathbb{R}, \qquad k = 1, 2, \ldots, m,$$

takes the form

$$(L_n)_k(\mathbf{x}) = (L_n)_k(x_1, x_2, \ldots, x_m) = \sum_{j=1}^{N} c_{kj} f_n^*(x_1 - x_{1j}) f_n^*(x_2 - x_{2j}) \ldots f_n^*(x_m - x_{mj}), \quad (14)$$

where

$$f_n^*(x_i - x_{ij}) = a\sqrt{\frac{n}{3}}\, f_n\left(a\sqrt{\frac{n}{3}}\,(x_i - x_{ij})\right), \qquad i = 1, 2, \ldots, m.$$

Here f_n *is given in (5),* n *is even,* $(x_1, x_2, \ldots, x_m)$ *is any point in* $\mathbb{R}^m$*, and* $(x_{1j}, x_{2j}, \ldots, x_{mj})$ *is a data site.*

Referring to Definition 4.1, we observe that the transformation function $(L_n)_k : \mathbb{R}^m \to \mathbb{R}$ has to be calculated for each $k = 1, 2, \ldots, m$, and the parameters c_{kj} in (14) are to be obtained by solving m systems of linear equations.

Since we are mainly interested in the bivariate transformation $\mathbf{L}_n : \mathbb{R}^2 \to \mathbb{R}^2$, we take $m = 2$ in (13), requiring that $\mathbf{L}_n$ solves Problem 2.1. Therefore, we have to consider

$$(L_n)_k(\mathbf{x}) = (L_n)_k(x_1, x_2) = \sum_{j=1}^{N} c_{kj} f_n^*(x_1 - x_{1j}) f_n^*(x_2 - x_{2j}),$$

which, imposing the conditions $(L_n)_1(\mathbf{x}_i) = t_{1i}$ and $(L_n)_2(\mathbf{x}_i) = t_{2i}$, for $i = 1, 2, \ldots, N$, gives two associated linear systems.

5 Numerical results

In this section we show the applicability of Lobachevsky transformations, referring to examples given in [12] and [14] which concern the registration of elastic images (see [2]). With respect to rigid or affine registration techniques, in which we have rigid objects embedded in elastic material changing their position or form, the approach we propose can handle successfully local differences between corresponding images. In general, these differences may be caused by the physical deformation of human tissue due to surgeries or pathological processes such as tumor growth or tumor resection.

The considered examples simulate typical medical cases, where image portions shift or scale. We denote with $\mathcal{X}$ the grid point set, which is formed by 40×40 points. The grid is transformed using 32 (case 1) and 64 (case 2) landmarks. Moreover, when a square is shifted, 4 quasi–landmarks are added to prevent an overall shift. The source and target image landmarks, shown in Figure 1 and in Figure 2 for both cases, are marked by a circle ($\circ$) and a star ($\star$), respectively.

Our aim is to determine a transformation function which connects the points of the two images, so that the target image is affected by the slightest possible deformation. In order to verify the goodness of the proposed spline transformations, we make a comparison of registration results using also Gaussian and thin plate spline transformations. Figures 3, 4, 5, and 6 show Lobachevsky, Gaussian and thin plate spline registration results (left to right), taking $\alpha = 1$ as shape parameter in the first two cases. Furthermore, in Tables 1, 2, 3, and 4 we report the root mean squares errors (RMSEs) and the maximum absolute errors (MAEs) obtained by using Lobachevsky spline transformations for $n = 2, 4, 6$ (denoted with L2, L4 and L6, respectively),

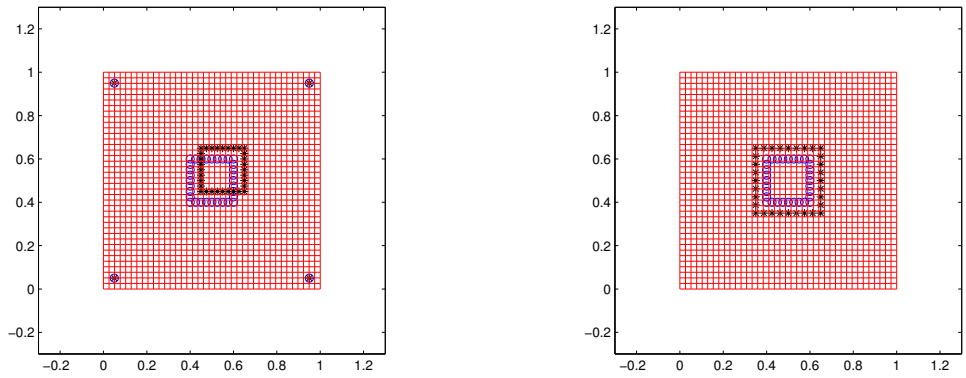

Figure 1: Square shift (left) and square scaling (right): source ($\circ$) and target ($\star$) landmarks (case 1).

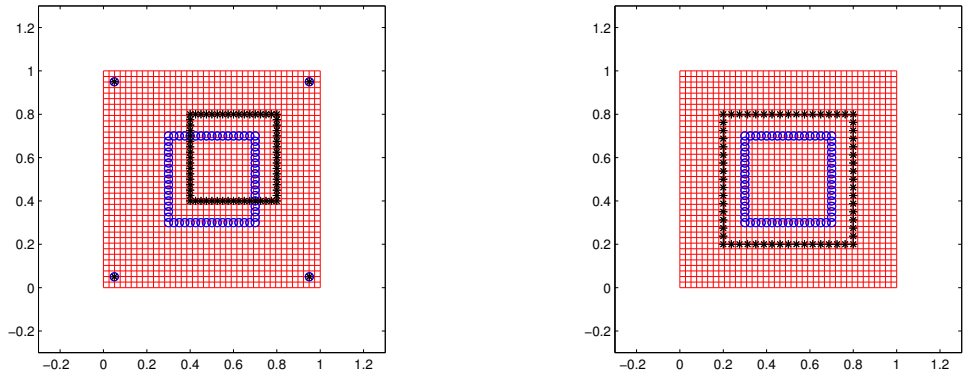

Figure 2: Square shift (left) and square scaling (right): source ($\circ$) and target ($\star$) landmarks (case 2).

Gaussian (G) and thin plate spline (TPS) transformations. These errors are found computing the distances between the displacements of grid points $x \in \mathcal{X}$ and the values obtained by the transformations. They assume the following form

$$\text{RMSE} = \sqrt{\frac{\sum_{\mathbf{x}\in\mathcal{X}} \|\mathbf{x} - \mathbf{F}(\mathbf{x})\|^2}{\sum_{\mathbf{x}\in\mathcal{X}} 1}}, \qquad \text{MAE} = \max_{\mathbf{x}\in\mathcal{X}} \|\mathbf{x} - \mathbf{F}(\mathbf{x})\|,$$

where $\|\cdot\|$ is the Euclidean norm.

	L2	L4	L6	G	TPS
RMSE	4.4160E − 2	4.9751E − 2	5.1238E − 2	6.2166E − 2	4.3460E − 2
MAE	1.2155E − 1	7.0959E − 2	7.0717E − 2	7.5323E − 2	7.1871E − 2

Table 1: Shift of a square: errors for $\alpha = 1$ (case 1).

We note that for square shifts Lobachevsky and thin plate spline transformations give grids which are visibly less deformed in comparison with Gaussian transformed grids, while for square

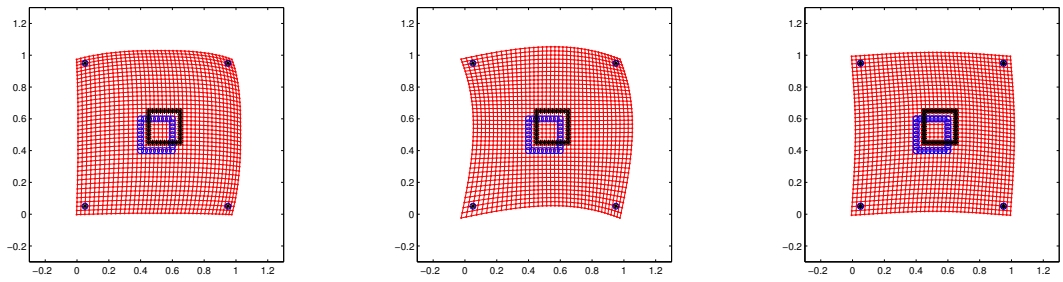

Figure 3: Shift of a square (case 1): registration results obtained by Lobachevsky splines L4 (left), Gaussian functions (center) with $\alpha = 1$, and thin plate splines (right).

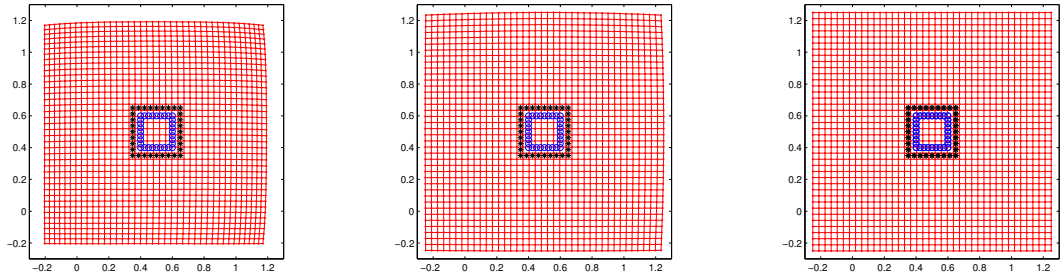

Figure 4: Scaling of a square (case 1): registration results obtained by Lobachevsky splines L6 (left), Gaussian functions (center) with $\alpha = 1$, and thin plate splines (right).

	L2	L4	L6	G	TPS
RMSE	2.8312E − 1	1.3931E − 1	1.8271E − 1	2.0763E − 1	2.0929E − 1
MAE	7.5136E − 1	2.2327E − 1	2.8785E − 1	3.4941E − 1	3.5355E − 1

Table 2: Scaling of a square: errors for $\alpha = 1$ (case 1).

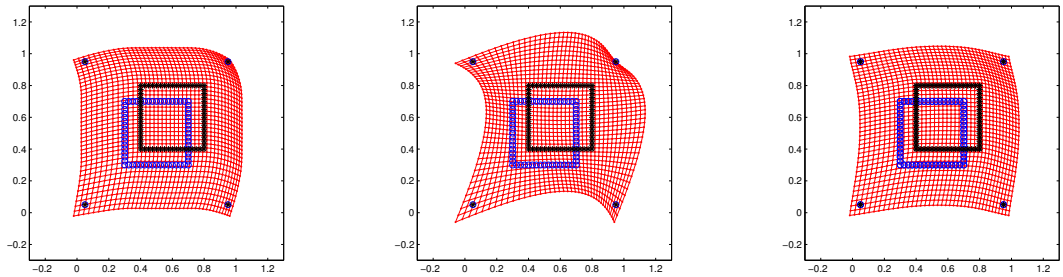

Figure 5: Shift of a square (case 2): registration results obtained by Lobachevsky splines L4 (left), Gaussian functions (center) with $\alpha = 1$, and thin plate splines (right).

scaling registration the results of Lobachevsky transformations are significantly better, since grid deformations are limited. Moreover, registration errors point out that Lobachevsky transformations are comparable and sometimes better than those obtained with the radial basis function

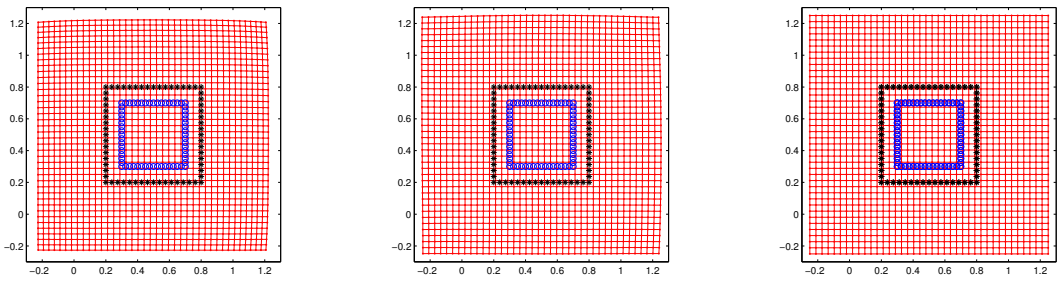

Figure 6: Scaling of a square (case 2): registration results obtained by Lobachevsky splines L6 (left), Gaussian functions (center) with $\alpha = 1$, and thin plate splines (right).

	L2	L4	L6	G	TPS
RMSE	9.6830E − 2	1.0335E − 1	1.1182E − 1	1.3666E − 1	1.0310E − 1
MAE	1.4142E − 1	1.4164E − 1	1.4169E − 1	1.8994E − 1	1.5131E − 1

Table 3: Shift of a square: errors for $\alpha = 1$ (case 2).

	L2	L4	L6	G	TPS
RMSE	1.5291E − 1	1.7152E − 1	1.9817E − 1	2.0849E − 1	2.0929E − 1
MAE	5.1545E − 1	2.6796E − 1	3.1900E − 1	3.4929E − 1	3.5355E − 1

Table 4: Scaling of a square: errors for $\alpha = 1$ (case 2).

approach.

Quantitative graphs for the accuracy of the registration results are shown in Figure 7 and Figure 8, where the RMSEs obtained by varying the parameter α in Lobachevsky splines and Gaussians are presented. Thus, exploiting the analysis of errors in Figure 7 and Figure 8, we can take good values for α and compare the registration results, obtained by applying Lobachevsky and Gaussian functions. Their comparison points out the goodness and the effectiveness of our approach. In particular, such graphs point out that Lobachevsky splines (at least for $n = 2, 4, 6$) produce better registration results than Gaussian functions for equispaced values of $\alpha \in [0.1, 2.0]$.

Finally, in Table 5 we report condition numbers of interpolation matrices. We observe that condition numbers of Lobachevsky splines are generally much smaller than those of the Gaussian but larger, except $L2$, than the condition numbers of thin plate splines.

	L2	L4	L6	G	TPS
Shift (case 1)	4.8918E + 03	2.7992E + 09	1.0031E + 13	2.3082E + 17	3.0583E + 04
Shift (case 2)	6.7668E + 04	1.5389E + 09	6.3546E + 12	2.2036E + 18	5.3148E + 04
Scaling (case 1)	6.9016E + 04	2.5711E + 09	9.1953E + 12	2.0573E + 17	2.6722E + 04
Scaling (case 2)	6.5173E + 04	1.4710E + 09	6.0739E + 12	1.0419E + 19	5.0165E + 04

Table 5: Condition numbers for $\alpha = 1$.

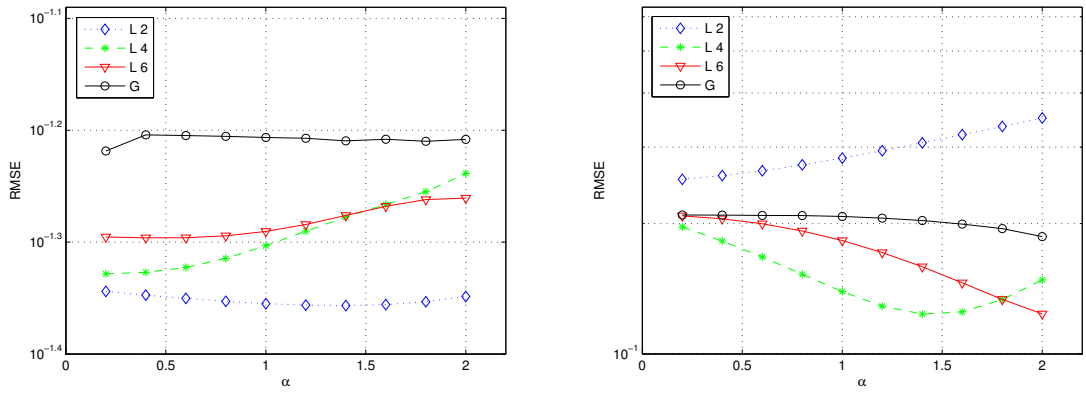

Figure 7: Shift (left) and scaling (right) of a square: RMSEs using Lobachevsky splines L2, L4, L6, and Gaussian functions by varying the shape parameter α (case 1).

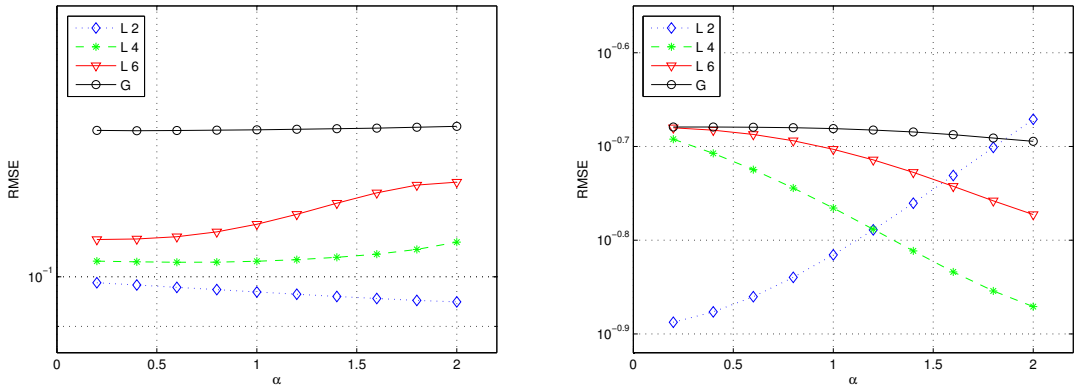

Figure 8: Shift (left) and scaling (right) of a square: RMSEs using Lobachevsky splines L2, L4, L6, and Gaussian functions by varying the shape parameter α (case 2).

6 An application to a real-life case

In this section we present experimental results obtained by applying Gaussian, thin plate spline and Lobachevsky spline schemes to real image data. More precisely, we consider two X-ray images of the cervical of an anonymous patient taken at different times. In Figure 9 we show the two images along with landmarks and quasi-landmarks, setting on the left the source image and on the right the target one. The size of both images is 512×512 pixels. In particular, within each of the two images we have manually selected 6 landmarks. Moreover, to fix transformation and to prevent an overall shift, we have added 12 quasi-landmarks on the boundaries of the source and target images.

Each result in Figure 10 (a), (b), (c) and (d) represents a transformed image, obtained using Gaussian, thin plate and Lobachevsky spline tranformations, respectively. For the Gaussian and Lobachevsky L4 and L6 spline transformations we have used the parameter value $\alpha = 1.6$. We observe that the Gaussian transformation strongly deforms the image, while thin plate splines and Lobachevsky splines give significantly better results, since deformations are limited and the transformed images are very similar to the target image.

Moreover, for Lobachevsky splines (L2, L4 and L6) and Gaussians we have analyzed the behaviour of registration results obtained by varying the value of $\alpha \in [0.1, 2.0]$. This allows

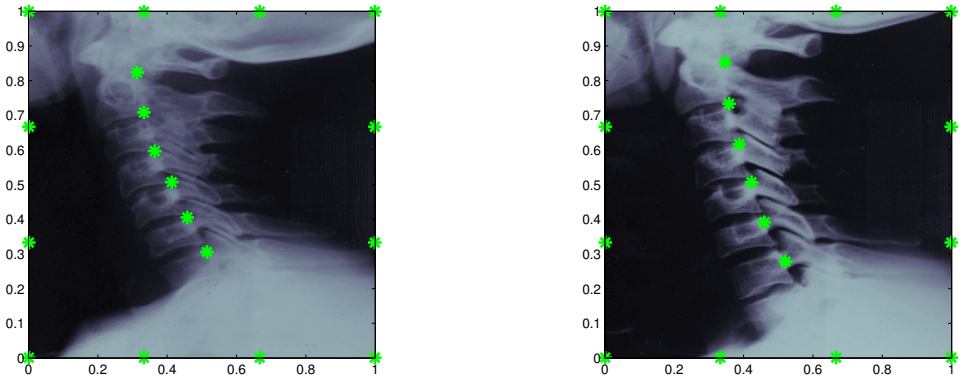

Figure 9: Source and target cervical images with landmarks and quasi-landmarks (left to right).

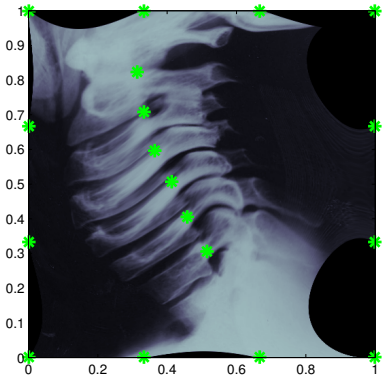

(a) G, $\alpha = 1.6$

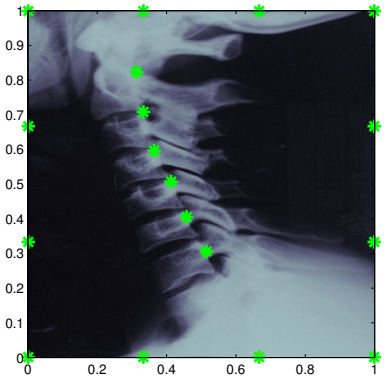

(b) TPS

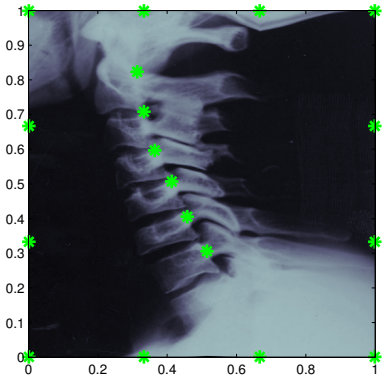

(c) L4, $\alpha = 1.6$

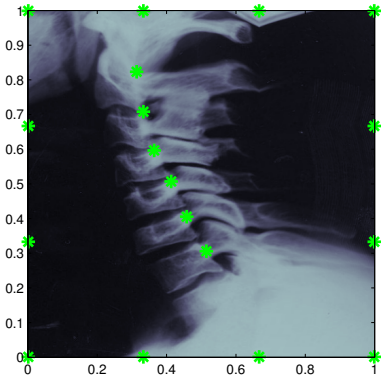

(d) L6, $\alpha = 1.6$

Figure 10: Registration results obtained by Gaussian (a), thin plate spline (b) and Lobachevsky spline (c)-(d) for the cervical image.

us to note that: (i) L2 gives similar results for every value of α; (ii) L4 produces a slight deformation at the bottom of the transformed image when $\alpha < 1.6$, whereas results similar to those shown in Figure 10 (c) are obtained when $\alpha \geq 1.6$; (iii) L6 provides a slight deformation at the bottom of the transformed image when $\alpha < 1.2$, while results similar to those pointed out in Figure 10 (d) are obtained when $\alpha \geq 1.2$; (iv) G does not produce good registration results

for any value of α and the transformed image is strongly deformed; furthermore, for $\alpha < 0.4$ interpolation matrices turn out to be ill-conditioned. Note that this drawback does not occur using Lobachevsky splines.

7 Conclusions

In this paper we have proposed the use of a class of piecewise polynomials, called Lobachevsky splines, in the context of landmark-based image registration. After deducing analytic expressions of Lobachevsky splines, using concepts of probability theory, we have presented their noteworthy properties, like the convergence of sequences of Lobachevsky splines to the normal density function (i.e., Gaussian function) and the convergence of sequences of their integrals and derivatives. Moreover, Lobachevsky splines of each even degree $n \geq 2$ are strictly positive definite functions, and, being compactly supported, they produce sparse interpolation matrices (for suitable choices of shape parameters) and fast evaluation. Furthermore, Lobachevsky splines generate interpolation matrices whose condition numbers are generally much smaller than those of Gaussian transformations. Several numerical results have been carried out by considering typical test cases: they have shown that Lobachevsky splines are usually more accurate and stable than Gaussians (in particular, referring to RMSEs and condition numbers), and at the same time are comparable with thin plane splines. Finally, an application to cervical X-ray images has pointed out good applicability and effectiveness of Lobachevsky spline transformations in landmark-based registration. This has also been supported by a comparison with Gaussian and thin plate spline transformations.

Acknowledgements

The authors kindly thank the Department of Mathematics "G. Peano"– University of Turin for its financial support through the project "Modelling and approximation of complex systems (2010)". The work of the second author has been performed with a grant of the "Istituto Nazionale di Alta Matematica" (INdAM), which is gratefully acknowledged.

References

[1] Allasia G. Scattered multivariate interpolation by a class of spline functions. In Vigo-Aguiar J et al (eds), *Proceedings of the 9th International Conference CMMSE09*, vol. 1, 2009; 73–79.

[2] Allasia G, Cavoretto R, De Rossi A, Quatember B, Recheis W, Mayr M, Demertzis S. Radial basis functions and splines for landmark-based registration of medical images. In Simos TE, Psihoyios G, Tsitouras C (eds), *Proceedings of the International Conference on Numerical Analysis and Applied Mathematics*. AIP Conference Proceedings, vol. 1281: Melville, New York, 2010; 716–719.

[3] Bookstein F. Principal warps: thin-plate splines and the decomposition of deformations. *IEEE Transactions on Pattern Analysis and Machine Intelligence* 1989; **11**:567–585.

[4] Brinks R. On the convergence of derivatives of B-splines to derivatives of the Gaussian functions. *Computational & Applied Mathematics* 2008; **27**:79–92.

[5] Brown LG. A survey of image registration techniques. *ACM Computing Surveys* 1992; **24**:325–376.

[6] Cavoretto R, De Rossi A. A local IDW transformation algorithm for medical image registration. In Simos TE, Psihoyios G, Tsitouras C (eds), *Proceedings of the International Conference of Numerical Analysis and Applied Mathematics*. AIP Conference Proceedings, vol. 1048: Melville, New York, 2008; 970–973.

[7] Cavoretto R, De Rossi A, Quatember B. Landmark-based registration using a local radial basis function transformation. *Journal of Numerical Analysis, Industrial and Applied Mathematics* 2011; **5**:141–152.

[8] Cavoretto R. *Meshfree Approximation Methods, Algorithms and Applications*. PhD Thesis, University of Turin, 2010.

[9] Cheney EW, Light W. *A Course in Approximation Theory*. Brooks Cole: Pacific Grove, CA, 1999.

[10] Fasshauer G. *Meshfree Approximation Methods with MATLAB*. World Scientific: Singapore, 2007.

[11] Feller W. *An Introduction to Probability Theory and its Application*, vol. 2, Wiley & Sons, New York, 1971.

[12] Fornefett M, Rohr K, Stiehl HS. Radial basis functions with compact support for elastic registration of medical images. *Image and Vision Computing* 2001; **19**:87–96.

[13] Gnedenko BV. *The Theory of Probability*. MIR: Moscow, 1976.

[14] Kohlrausch J, Rohr K, Stiehl HS. A new class of elastic body splines for nonrigid registration of medical images. *Journal of Mathematical Imaging and Vision* 2005; **23**:253–280.

[15] Lobachevsky N. Probabilité des resultats moyens tirés d'observations répetées. *Journal für die Reine und Angewandte Mathematik* 1842; **24**:164–170.

[16] Lukacs E. *Characteristic Functions*. Griffin: London, 1970.

[17] Lund J, Bowers KL. *Sinc Methods for Quadrature and Differential Equations*. SIAM: Philadelphia, PA, 1992.

[18] Maintz JBA, Viergever MA. A survey of medical image registration. *Medical Image Analysis* 1998; **2**:1–37.

[19] Maurer Jr. CR, Fitzpatrick JM. A review of medical image registration. In Maciunas RJ (ed), *Interactive Image-Guided Neurosurgery*. American Association of Neurological Surgeons: Park Ridge, 1993; 17–44.

[20] Medical Image Processing, Analysis and Visualization (MIPAV), software package, http://mipav.cit.nih.gov.

[21] Modersitzki J. *Numerical Methods for Image Registration*. Oxford University Press: Oxford, 2004.

[22] Modersitzki J. *FAIR: Flexible Algorithms for Image Registration*. Fundamentals of Algorithms 6, SIAM: Philadelphia, PA, 2009.

[23] Quatember B, Mayr M, Recheis W, Demertzis S, Allasia G, De Rossi A, Cavoretto R, Venturino E. Geometric modelling and motion analysis of the epicardial surface of the heart. *Mathematics and Computers in Simulation* 2010; **81**:608–622.

[24] Quatember B, Recheis W, Mayr M, Demertzis S, Allasia G, Cavoretto R, De Rossi A, Venturino E. Methods for accurate motion tracking and motion analysis of the beating heart wall. In Vigo-Aguiar J et al (eds), *Proceedings of the 10th International Conference CMMSE10*, vol. 4, 2010; 1222–1227.

[25] Rényi A. *Calcul des Probabilités*. Dunod: Paris, 1966.

[26] Rohr K. *Landmark-based Image Analysis, Using Geometric and Intensity Models*. Kluwer Academic Publishers: Norwell, MA, 2001.

[27] Schumaker LL. *Spline Functions: Basic Theory*. Krieger Publishing Company: Malabar, Florida, 1993.

[28] Stenger F. *Numerical Methods based on Sinc and Analytic Functions*. Springer Series in Computational Mathematics, vol. 20. Springer-Verlag: New York, 1993.

[29] Unser M, Aldroubi A, Eden M. On the asymptotic convergence of B-splines wavelets to Gabor functions. *IEEE Transactions on Information Theory* 1991; **8**:864–872.

[30] Van der Elsen PA, Pol EJD, Viergever MA. Medical image matching – A review with classification. *IEEE Engineering in Medicine and Biology Society* 1993; **12**:26–39.

[31] Wendland H. *Scattered Data Approximation*. Cambridge Monographs on Applied and Computational Mathematics, vol. 17. Cambridge University Press: Cambridge, 2005.